Summary of the “Diffraction & Vector Mesons” working group at DIS05

X. Janssen*, M. Ruspa† and V. A. Khoze**

*DESY, 22607 Hamburg, Germany
†University of Eastern Piedmont, 28100 Novara, Italy
**IPPP, University of Durham, DH1 3LE,UK

Abstract.
We survey the contributions presented in the working group: “Diffraction & Vector Mesons”.

Keywords: diffractive deep inelastic scattering, Pomeron, diffractive PDFs, factorization, vector mesons, DVCS, GPDs, diffractive Higgs
PACS: 13.60Hb, 13.60Le, 12.38Bx, 12.39St, 12.40Nn

INTRODUCTION

In diffractive interactions in hadron-hadron or photon-hadron collisions at least one of the beam particles emerges intact from the collision, having lost only a small fraction of its initial energy, and carrying a small transverse momentum. Therefore no color is exchanged in the t-channel. The signature for such processes is the presence of a gap in rapidity between the two hadronic final states. At high energy this is described by the exchange of an object with the quantum numbers of the vacuum, referred to as the Pomeron in the framework of Regge phenomenology [1]. Note that at low energies similar reactions can also proceed when quantum numbers are exchanged through subleading Regge trajectories (Reggeons); however, these contributions are exponentially suppressed as a function of the gap size and are negligible at small values of the longitudinal momentum loss. The understanding and description of diffractive processes is one of the aims of QCD.

Diffractive events are being extensively studied at HERA, TEVATRON, RHIC, JLAB and CERN and there is a growing community planning to continue these studies at the LHC. Updates on the available experimental data and on their theoretical interpretation were given at this workshop; many discussions also took place on the future plans. In the present summary we focus on the path from HERA to the LHC through the TEVATRON.

FROM HERA TO HADRON COLLIDERS

Selection of diffractive processes

Let us first look at the diffractive reaction $ep \to eXp$ at HERA, depicted in Fig. 1a: a photon of virtuality Q^2 diffractively dissociates interacting with the proton at a center

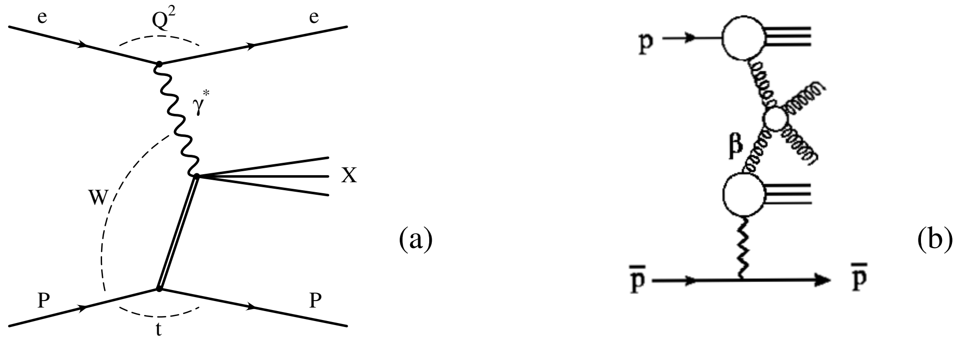

FIGURE 1. (a) Diffraction in ep interactions. (b) Diffraction in $p\bar{p}$ interactions.

of mass energy W and squared four momentum transfer t and produces the hadronic system X with mass M_X in the final state. The fraction of the proton momentum carried by the exchanged object is denoted by $x_{\mathbb{P}}$, while the fraction of the momentum of the exchanged object carried by the struck quark is denoted by β (note that sometimes z is used instead of β). The virtual photon emitted from the lepton beam provides a point-like probe to study the structure of the diffractive exchange, similarly to ordinary DIS probing proton structure. The fact that a large fraction ($\sim 10\%$) of deep inelastic (DIS) events at HERA is diffractive has thus opened the possibility of investigating the partonic nature of the Pomeron and has established a theoretical link between Regge theory and QCD.

At the TEVATRON inclusive diffraction is mainly studied via the reaction $p\bar{p} \rightarrow \bar{p}X$, sketched in Fig. 1b; in the TEVATRON jargon $x_{\mathbb{P}}$ is usually indicated as ξ.

At HERA three methods are used to select diffractive events [2]. The first is based on the measurement of the scattered proton with a spectrometer installed very close to the beam in a region with acceptance for protons which have lost only a small fraction of their initial longitudinal energy. A second method requires the presence of a large rapidity gap (LRG) in the forward region. A third method is based on the different shape of the M_X distribution between diffractive and non diffractive events. At the TEVATRON diffractive interactions are selected by tagging events by either a rapidity gap or a leading antiproton [3].

The proton tagging method has the advantage of excluding the proton dissociation processes $ep \rightarrow eXN$, where the proton also diffractively dissociates into a state N of mass M_N that escapes undetected into the beam pipe. In order to ensure that the scattered proton resulted from a diffractive process one requires $x_{\mathbb{P}} < 0.01$. This cut removes contributions coming from Reggeon exchanges [4].

The large rapidity gap method selects events which include some proton dissociation processes and some Reggeon contributions. The latter can be removed by the same $x_{\mathbb{P}}$ cut as above. If the mass M_N of the dissociative system is large enough to be measured in the forward detector the proton dissociation background can be removed, whereas the contribution of low mass proton dissociation can be estimated with a Monte Carlo simulation (10% of background with $M_N < 1.6$ GeV is quoted from the H1 analysis [5]).

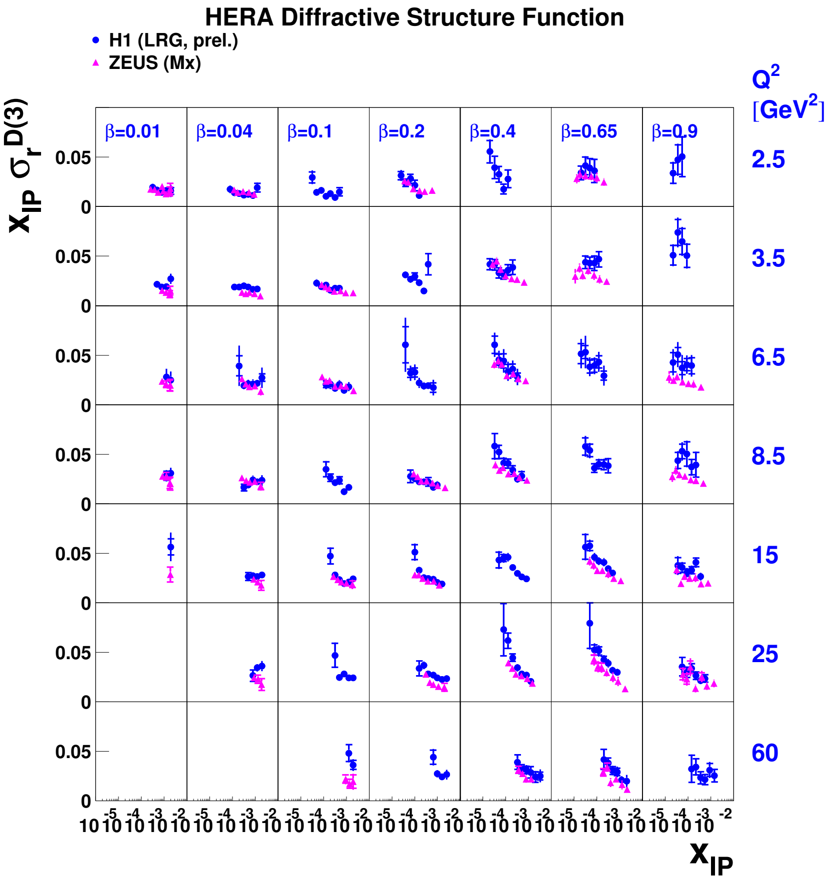

FIGURE 2. ZEUS M_X and H1 LRG measurements of the diffractive structure function.

In the M_X method the statistical subtraction of the non diffractive background eliminates also the the Reggeon contribution, but the selected sample is left with an important contamination from proton dissociative events with masses $M_N < 2.3$ GeV [6]. By comparing the measured cross sections with those coming from the leading proton analysis one can estimate the amount of this background (around 30% [7]) and determine a correction factor.

HERA diffractive structure function and PDFs

H1 and ZEUS have presented recent precise measurements of the diffractive structure function obtained with all three HERA methods and covering a wide kinematic range (proton tagging method: [2, 8], LRG method: [5], M_x method: [6]). In Fig. 2 the diffractive structure function is presented as a function of x_{IP} for fixed values of Q^2 and β. The data points come from two samples analysed by H1 with the LRG method and by ZEUS with the M_X method, respectively. The ZEUS M_X data have been scaled to $M_Y < 1.6$ GeV, the region of dissociative masses included in the H1 data. There is

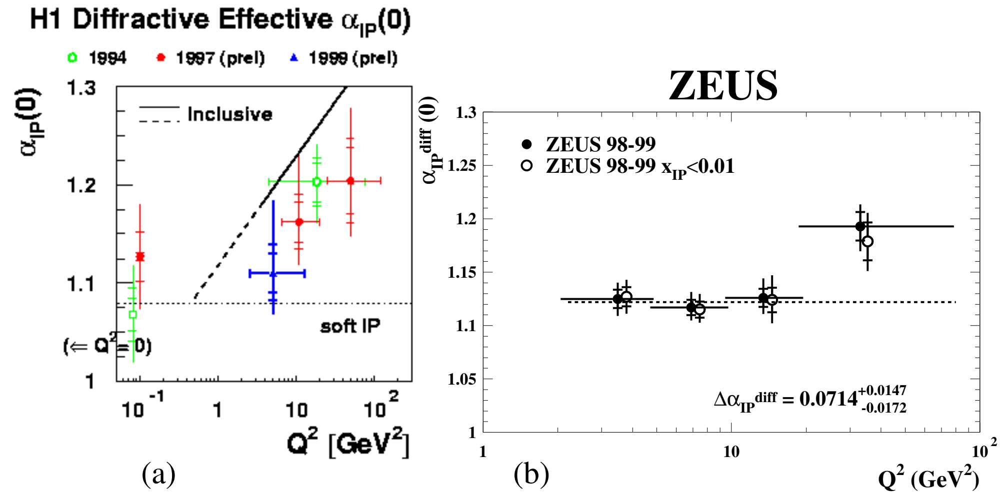

(a) (b)

FIGURE 3. Q^2 dependence of the Pomeron intercept $\alpha_{I\!P}(0)$, measured by H1 (a) and by ZEUS (b).

a reasonable agreement between the two data sets, but at a closer inspection it turns out that the Q^2 dependences are different, namely the positive scaling violations in the ZEUS data are smaller than in the H1 data. This discrepancy has been investigated very recently by a combined set of next-to-leading-order (NLO) QCD fits of the diffractive structure function, attempted by two different groups (P. Newman et al. [9] and A. Levy et al. [10] - see also the upcoming proceedings of the HERA-LHC workshop, http://www.desy.de/∼heralhc).

Such fits are based on the validity of a collinear factorization theorem in diffractive processes [11], which allows to write F_2^D as a convolution of the usual partonic cross sections as in DIS with diffractive parton distribution functions (DPDFs). The DPDFs, parametrised at a starting scale, are evolved according to the DGLAP equations [12] and fitted to the data. In the ideal case we would evolve in Q^2 for fixed t and x_{IP}, or at least for fixed x_{IP} if t is integrated over, but this is not allowed by the rather limited statistics of the present data. An alternative approach is the assumption, known as "Regge factorization" hypothesis, that F_2^D can be expressed as the product of a flux, depending only on x_{IP} and t, and the structure function of a particle-like object. Whether the data support this assumption or not is a controversial problem. It translates into determining whether or not the intercept $\alpha_{I\!P}(0)$ of the Pomeron trajectory $\alpha_{I\!P}(t) = \alpha_{I\!P}(0) + \alpha' t$ depends on Q^2.

Fig. 3a shows $\alpha_{I\!P}(0)$ as a function of Q^2, as measured by H1 : there is a suggestion of a dependence of $\alpha_{I\!P}(0)$ on Q^2, though firm conclusions are not possible with the present uncertainties. In Fig. 3b, where the ZEUS measurement is presented, the Pomeron intercept rises by $\Delta\alpha_{\mathrm{diff}} = 0.0741 \pm 0.0140(\mathrm{stat.})^{+0.0047}_{-0.0100}(\mathrm{syst.})$ between Q^2 of 7.8 GeV^2 and 27 GeV^2, with a significance of 4.2 standard deviations. This scenario suggests a possible violation of Regge factorization and a clear need for more precise data. Nevertheless it has been shown [10] that, when restricting the analysed range to $x_{IP} < 0.01$, Regge factorization is a sufficiently good approximation and this is the compromise at the basis of the NLO DGLAP fits discussed in the following.

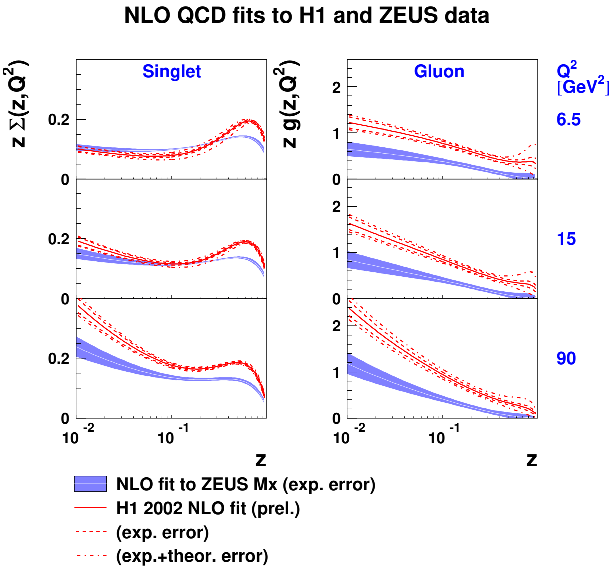

FIGURE 4. The diffractive parton densities resulting from a NLO QCD fit by P. Newman et al. [9] to the ZEUS M_X data (solid line) and to the H1 LRG data (shaded line).

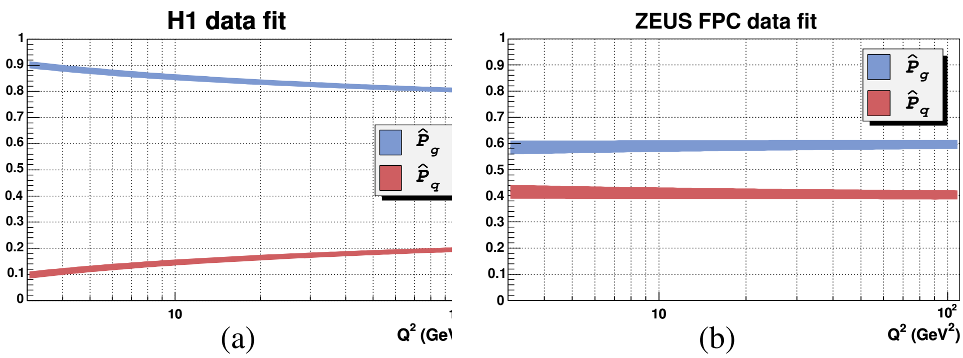

FIGURE 5. The parton momentum fraction as a function of Q^2 from a NLO QCD fit by A. Levy et al. [10] to the H1 LRG data (a) and to the ZEUS M_X data (b).

In Fig. 4 a comparison is shown between the diffractive PDFs extracted from the NLO QCD fit by P. Newman et al. to the ZEUS M_X data (solid line) and from the same fit to the H1 LRG data (shaded line), the latter being essentially the well known H1 fit 2002 [5]. Note that most of the data points from the high β region, where discrepancies arise between the data sets (Fig. 2), have not been included in the fit. As a reflection of the difference in the scaling violations between the two sets of measurements (Fig. 2), the quark density is similar at low Q^2 and evolves differently to higher Q^2; the gluon density is a factor ~ 2 smaller in the ZEUS data than in the H1 sample. This disagreement is confirmed and quantified in Fig. 5, which shows the fraction of the Pomeron momentum carried by quarks (red/dark line) and by gluons (blue/light line), as a function of Q^2, as resulting from the fit by A. Levy et al., similar to the previous one, but completely independent, performed always on the H1 LRG data (Fig. 5a) and on the ZEUS M_X data

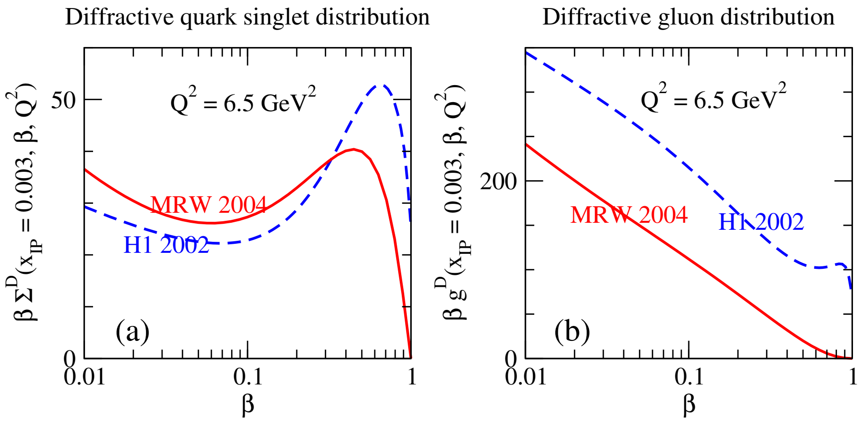

FIGURE 6. The diffractive parton densities resulting from a combined QCD fit by A. Martin et al. [13] to the ZEUS proton tagged, ZEUS M_X and H1 LRG data. The dashed lines are the densities obtained in the H1 fit 2002 [5].

(Fig. 5b). The fraction of the Pomeron momentum carried by gluons turns to be between 70% and 90% in the H1 data and between 55% and 65% in the ZEUS M_X data. The same study has been carried out also on the ZEUS proton tagged data and the resulting integral of the fractional momentum is in agreement with the H1 value.

The same data have also been analysed according to a new approach by A. Martin et al. [13], which does not assume Regge factorization and shows that the collinear factorization theorem, though valid asymptotically in diffractive DIS, has important modifications at the energies relevant at HERA, which can be quantified using perturbative QCD. The DPDFs are shown to satisfy an inhomogeneous evolution equation and the need of including both the gluonic and sea-quark components of the perturbative Pomeron is considered. The DPDFs resulting from a combined fit to the ZEUS proton tagged data and M_X data and to the H1 LRG data are shown in Fig. 6 (solid line), together with H1 fit 2002 (dashed line). While the quark densities are not very different from those of H1, the gluon distribution is significantly lower than H1 one.

The discrepancies between the various DPDFs shown in Figs. 4 and 6 are large and presently not fully understood. They are due to a combination of effects: disagreement in the data, different fit methods and assumptions behind them. Therefore these very differences between the DPDFs are at the moment the only realistic estimate we have of their uncertainties. A precise and consistent determination of the DPDFs is certainly one of the main tasks that the HERA community has to face in the near future. Among other reasons, they are a crucial input for the prediction of any inclusive diffractive cross section at the LHC.

QCD factorization tests

According to the factorization theorem, calculations based on DPDFs extracted from inclusive measurements should allow to predict cross sections for other diffractive pro-

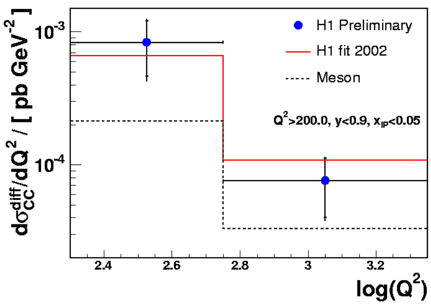

FIGURE 7. H1 charge current differential cross section $d\sigma_{cc}^{diff}/dQ^2$ as a function of $log(Q^2)$.

cesses. Calculations based on H1 fit 2002 agree well with the data on diffractive D^* production in DIS [14] and diffractive dijet production in DIS [15]. A further test of factorization comes from the study of events with a large rapidity gap in charged current interactions at high Q^2: in Fig. 7 the differential cross section $d\sigma_{cc}^{diff}/dQ^2$, as measured by H1 [16], is presented as a function of Q^2 and is well described by a calculation based on H1 fit 2002. A similar result was obtained by ZEUS [17]. However, the important uncertainties on the DPDFs discussed in the previous section make the conclusions on the validity of QCD factorization in DIS rather weak.

The factorization theorem does not hold in the case of diffractive hadron-hadron scattering [11]: indeed it has been known for years that the DPDFs extracted from HERA data overestimate the rate of diffractive dijets at the TEVATRON by one order of magnitude [18]. It was shown in [19] that this breakdown of factorization can be explained by screening (unitarization) effects. In the t-channel Reggeon framework, these effects are described by multi-Pomeron exchange diagrams. Because of the screening, the probability of rapidity gaps in high energy interactions to survive decreases since they may be populated by rescattering processes. The screening corrections are accounted for by the introduction of a suppression factor, which is often called the *survival probability of rapidity gaps*. As shown in [19] and [20], the current CDF diffractive dijet data, with one or two rapidity gaps, are in good quantitative agreement with the multi-Pomeron-exchange model.

In photoproduction at HERA ($Q^2 \sim 0$), the exchanged photon, which is real or quasi real, can either interact directly with the proton or first dissolve into partonic constituents which then scatter off the target (resolved process). In the former case dijet photoproduction is described by a photon gluon fusion process. In the latter case the photon behaves like a hadron. Factorization should then be valid for direct interactions as in the case of DIS with large Q^2, whereas for the resolved contribution it is expected to fail due to rescattering corrections. In the ideal theoretical limit, the suppression factor of 0.34 is evaluated for the resolved process within the multi-Pomeron exchange model [21]. However, in reality there is no clear model independent separation between the direct and resolved processes. In particular, the direct contribution is smeared by the experimental resolution and uncertainties. Moreover, at NLO these contributions are closely related. Recently Klasen and Kramer [22] have performed an analysis of diffractive dijet photoproduction data at NLO where they suppressed the resolved process by a factor 0.34.

Fig. 8 shows the differential cross section, as measured by H1 [15], for the diffractive photoproduction of two jets as a function of x_γ (the fraction of the photon momentum entering the hard scattering), where the NLO prediction has been tested in two different weighting schemes: in Fig. 8a only the resolved part has been scaled by the factor 0.34, while in Fig. 8b a global suppression factor 0.5 is applied to both the direct and resolved components. In Fig. 9 the ratio of the ZEUS data [23] to the NLO predictions of Klasen and Kramer [22] with no suppression factor ($R = 1$) is shown separately for the sample enriched (a) in the direct ($x_\gamma \geq 0.75$) and (b) in the resolved ($x_\gamma < 0.75$) components. Both for resolved and direct photoproduction the ratio is flat, but the data are lower by a factor of ~ 2 compared to the NLO calculations. Deviations are seen in E_T^{jet1} and in η^{jet1}, which are know to be sensitive to the structure function of the photon [24]. The overall message from the data of Figs. 8 and 9 is that, while a suppression of only the resolved contribution at NLO is disfavored by the data, a good agreement is achieved with the global suppression 0.5, which furthermore yields a good description of all measured cross sections.

The fact that the data, apparently against expectations, support suppression of direct photoproduction, has been addressed by M. Klasen [25] and has been related to the critical role of an initial state singularity in the way factorization breaks down and to the need of a modification of the suppression mechanism: separation of direct and resolved photoproduction events is a leading order concept. At NLO they are closely connected. The sum of both cross sections is the only physical relevant observable, which is approximately independent of the factorization scale, M_γ [26]. By multiplying the resolved cross section with the suppression factor $R = 0.34$, the scale dependence of the NLO direct cross section is compensated against that of the LO resolved part [22]. But at NLO collinear singularities arise from the photon initial state, which are absorbed at the factorization scale into the photon PDFs; the latter become in turn M_γ dependent. An equivalent M_γ dependence, just with the opposite sign, is then left in the NLO corrections to the direct contribution. Hence, in order to get a physical cross section at NLO, that is the superimposition of the NLO direct and LO resolved cross section, and to restore the scale invariance, one must multiply the M_γ dependent term of the NLO correction to the direct contribution with the same suppression factor as the resolved cross section.

The situation with the factorization breaking in dijet photoproduction is not completely clear and further experimental and theoretical efforts are needed. As was emphasized in [21], a possible way to study the effects of factorization breaking due to rescattering in diffractive photoproduction is to measure the ratio of diffractive and inclusive dijet photoproduction as a function of x_γ. In such quantity (at least) some of the theoretical and experimental uncertainties will cancel.

The understanding of factorization breaking in hadron-hadron collisions is of fundamental importance for the diffractive physics at the LHC. The rapidity gap survival factor is an essential ingredient of the predictions [27] on exclusive diffractive Higgs production, which will be discussed in the last section.

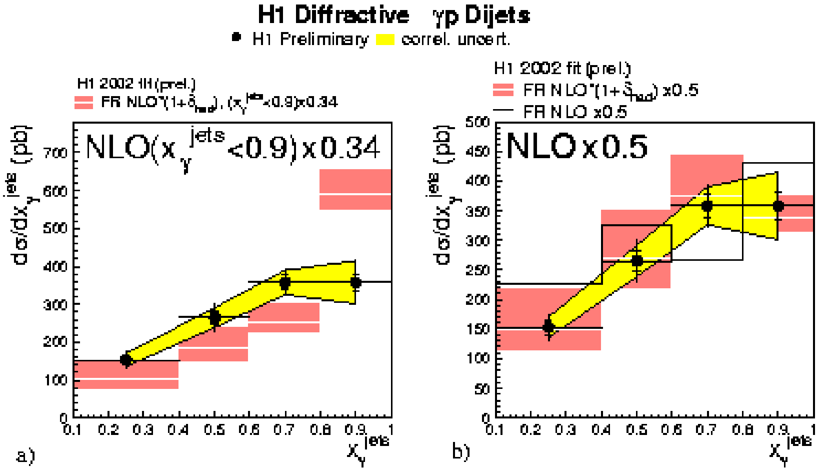

FIGURE 8. H1 cross section for the diffractive production of dijets in photoproduction as a function of x_{γ}. In (a) only the resolved contribution to the NLO calculation has been scaled by the factor 0.34, while in (b) the complete prediction is multiplied by a factor 0.5.

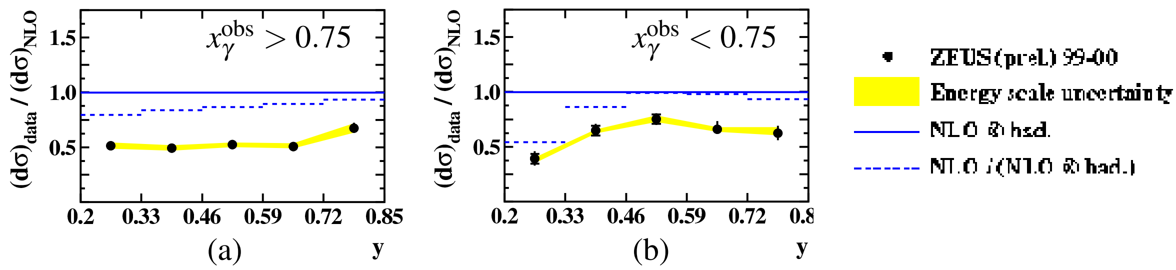

FIGURE 9. Ratio of the ZEUS diffractive dijet data to the NLO QCD predictions [22] of the single differential cross section in y for the sample enriched in direct (a) and resolved (b) photoproduction.

Diffraction at the TEVATRON

As discussed in the previous section, factorization is not expected to hold in hadron-hadron collisions. A strong breakdown of factorization at the TEVATRON has been known for some time from run-I (1992-1995) results [28]: the single-diffractive to non-diffractive ratios for dijets, W, b-quark and J/ψ production, as well as the ratio of double-diffractive to non-diffractive dijet production are all $\sim 1\%$, a factor 10 less than at HERA. However, the ratio of double- to single-diffractive dijets is found to be about a factor 5 larger than the ratio of single- to non-diffractive dijets, suggesting that there is only a small extra suppression when going from one to two rapidity gaps in the event, as confirmed by predictions [20]. In this respect the TEVATRON data are being a very powerful tool to shed light on the factorization breaking mechanism.

One of the major challenges of run-II is the measurement of central exclusive production rates (dijets, χ_c^0, diphotons). By central exclusive, we refer to the process $p\bar{p} \rightarrow p \oplus \phi \oplus \bar{p}$, where $\oplus$ denotes the absence of hadronic activity ('gap') between

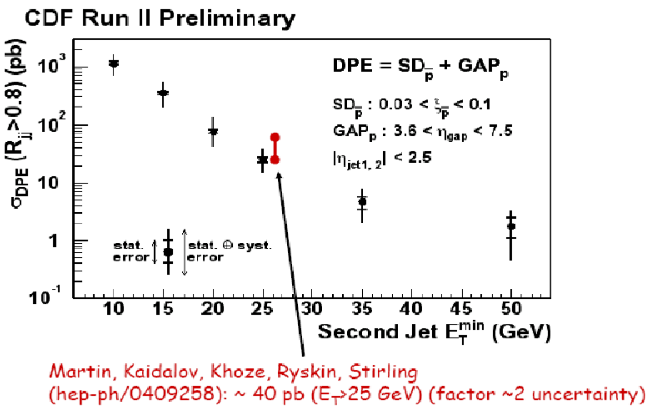

FIGURE 10. CDF dijet production cross section for $R_{jj} > 0.8$ in double Pomeron exchange events as a function of E_T^{min}, the E_T of the lower E_T jet.

the outgoing hadrons and the decay products of the central system ϕ. As we will discuss in the last section, the exclusive Higgs signal is particularly clean and the signal-to-background ratio is especially favorable, in comparison with other proposed selection modes. However, the expected number of events is low. Therefore it is important to check the predictions for exclusive Higgs production by studying processes mediated by the same mechanism, but with rates which are high enough to be observed at the TEVATRON (as well as at the LHC) [29].

The CDF search for exclusive dijet production is based on the reconstruction of the dijet mass fraction R_{jj} in double Pomeron exchange events. R_{jj} is defined as the mass of the two leading jets in an event divided by the total mass measured in all calorimeters. At first sight, we might expect that the exclusive dijets form a narrow peak concentrated at R_{jj} close to 1. In reality, the peak is smeared out due to hadronization and jet searching procedure as well as due to a 'radiative tail' phenomenon [30]. So it is not so surprising that within the CDF selection cuts no peak has been seen. CDF reports production cross sections for events with $R_{jj} > 0.8$, which are interpreted as the upper limits for exclusive production. Fig. 10 [28] shows such cross sections as a function of E_T^{min}, the E_T of the lower E_T jet. These data agree, within errors, with recent predictions for exclusive dijet production [29]. The analysis benefits from using dijet events in which at least one of the jets is b-tagged: presently more data on heavy flavor exclusive dijets are being collected with a special b-tagged dijet trigger.

Diffraction at RHIC

New interesting experimental results from RHIC were presented by Guryn, White and Klein. In particular, Guryn [31] described the results of the measurement of the single spin analyzing power A_N in polarized pp elastic scattering at 200 GeV. The recent results on inelastic diffraction with Au-Au, d-Au and pp beams were reviewed by White [32]. And Klein [33] showed the results of the STAR collaboration for coherent photonuclear ρ and 4 charged pion production.

Updates on theory

Several excellent mini review type theoretical talks were presented. Hard diffraction in DIS and the origin of hard Pomeron from rescattering were discussed by Brodsky [34]. He also reviewed such effects as Color Transparency, Color Opaqueness and Intrinsic Charm. Levin [35] gave a brief review of the current status of high density QCD with its ups and downs. The recent progress in the BFKL studies was covered by Andersen [36]. In particular, he discussed the high-energy limit of diffractive scattering processes in the BFKL resummation framework. He showed that the BFKL equation was solved at full next-to-leading logarithmic accuracy.

EXCLUSIVE MESON PRODUCTION AND DVCS

The dynamics of diffractive interactions can also be studied through exclusive vector meson ($V = \rho^0, \omega, J/\psi, ...$) and photon production, $l^\pm + N \longrightarrow l^\pm + V + Y$, where Y is either an elastically scattered nucleon or a low-mass state dissociative system. At low transverse momentum transfer at the nucleon vertex, the photoproduction of ρ^0, ω and ϕ mesons is characterized by a "soft" dependence of their cross-sections in the γp center-of-mass energy, W. This can be interpreted in the framework of Regge theory as due to the exchange of a "soft" Pomeron ($I\!P$) resulting in an energy dependence of the form $\mathrm{d}\sigma/\mathrm{dt} \propto \mathrm{W}^{4(\alpha_{\mathbf{P}}(\mathrm{t})-1)}$, where the Pomeron trajectory is parametrised as $\alpha_{I\!P}(t) = \alpha_{I\!P}(0) + \alpha' t \simeq 1.08 + 0.25t$. However, in the presence of a "hard" scale like large values of the photon virtuality Q^2or of the momentum transfer $|t|$ or of the vector meson mass, perturbative QCD (pQCD) is expected to apply. Diffractive vector meson production can then be seen in the nucleon rest frame as a sequence of tree subprocesses well separated in time: the fluctuation of the exchanged photon in a $q\bar{q}$ pair, the hard interaction of the $q\bar{q}$ pair with the nucleon via the exchange of (at least) two gluons in a color singlet state, and the $q\bar{q}$ pair recombination into a real vector meson. This approach results in a stronger rise of the cross section with W, which reflect the strong rise at small x of the gluon density in the nucleon. Such an energy dependence is observed in J/ψ production, where the quark charm mass provides a hard scale. It is of particular interest to study the role of other hard scales like Q^2 and t as well as the transition from a "soft" to "hard" behavior expected for light vector mesons. Furthermore, to take into account the skewing effect, i.e. the difference between the proton momentum fractions carried by the two exchanged gluons, one has to consider generalized parton distributions (GPDs). GPDs are an extension of standard PDFs, which include additional information on the correlations between partons and their transverse motion. There are four different types of GPDs, $H(x,x',t)$ and $E(x,x',t)$, where x and x' are the momentum fraction of the two parton considered, in the unpolarized case to which one should add $\tilde{H}(x,x',t)$ and $\tilde{E}(x,x',t)$ in the polarized case. While E and $\tilde{E}$ have no equivalent in the ordinary PDFs approach, H and $\tilde{H}$ reduce to the usual unpolarized and polarized PDFs respectively in the forward limit ($x = x'$ and $t = 0$).

The COMPASS experiment has presented [37] a study of the diffractive elastic leptoproduction of ρ^0 mesons, $\mu + N \longrightarrow \mu + \rho^0 + N$, where N is a quasi-free nucleon from any of the nuclei of their polarized target, at $< W >= 10$ GeV for a wide range of Q^2,

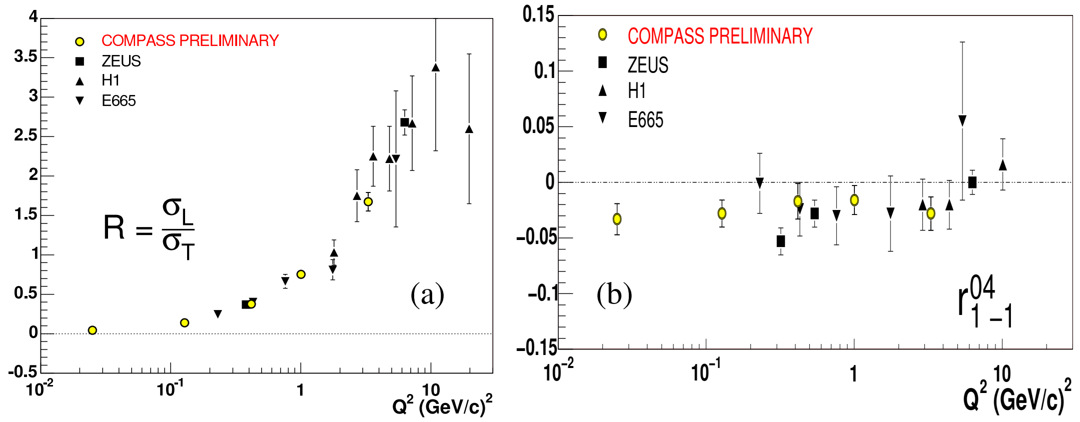

FIGURE 11. Q^2 dependence (a) of the ratio R between the longitudinal (σ_L) and the transverse (σ_T) cross sections and (b) of the r^{04}_{00} matrix element for elastic leptoproduction of ρ^0 as measured by COMPASS.

$0.01 < Q^2 < 10\,\mathrm{GeV}^2$. Several spin density matrix elements (SDME), which carry information on the helicity structure of the production amplitudes, have been extracted from the production and decay ρ^0 angular distributions. The COMPASS data provide a large statistics which allows to extend the previous measurements towards low Q^2. Measurements of the r^{04}_{00} matrix element, which can be interpreted as the fraction of longitudinal ρ^0 in the sample, have been performed as a function of Q^2. If one assumes s-channel helicity conservation (SCHC) between the exchanged photon and the ρ^0 meson, one can obtain the ratio R between the longitudinal (σ_L) and the transverse (σ_T) cross sections (see Fig. 11a). A weak violation of SCHC is observed through the r^{04}_{1-1} matrix element (see Fig. 11b, in agreement with results of previous experiments. It has to be noted that the study of systematic effects is still ongoing and that only the statistical errors are provided.

Elastic electroproduction of ϕ mesons has been studied in $e^{\pm}p$ collisions by the ZEUS experiment [38] in the kinematic range $2 < Q^2 < 70$ GeV^2, $35 < W < 145$ GeV and $|t| < 0.6$ GeV^2. The energy dependence of the $\gamma^* p$ cross section has been measured and can be parametrised as $\sigma \propto W^{\delta}$, with $\delta \simeq 0.4$. This value is between the "soft" diffraction value and the one observed for J/ψ. No Q^2 or t dependence of the slope δ was observed with the present precision. When parametrised as a falling exponential, the t dependence of the cross section leads to b slopes in the range from 6.4 ± 0.4 GeV^{-2} at $Q^2 = 2.4$ GeV^2 to 5.1 ± 1.1 GeV^{-2} at $Q^2 = 19.7$ GeV^2. The values of δ and b were found to scale with respect to other vector mesons results when plotted as a function of $Q^2 + m_V^2$, where m_V is the mass of the vector meson, suggesting that this could be a good approximation of the universal scale in this process. The ratio between the longitudinal (σ_L) and the transverse (σ_T) cross sections, extracted from the ϕ angular distributions, was found to increase with Q^2 and when compared with results obtained for other vector mesons to scale with Q^2/m_V^2.

H1 has presented [39] comprehensive results on elastic J/ψ production in the $\gamma^* p$ center-of-mass energy ranges $40 < W < 305$ GeV in photoproduction and $40 < W < 160$ GeV in electroproduction up to 80 GeV^2 in Q^2 and in both cases for $|t| < 1.2$ GeV^2.

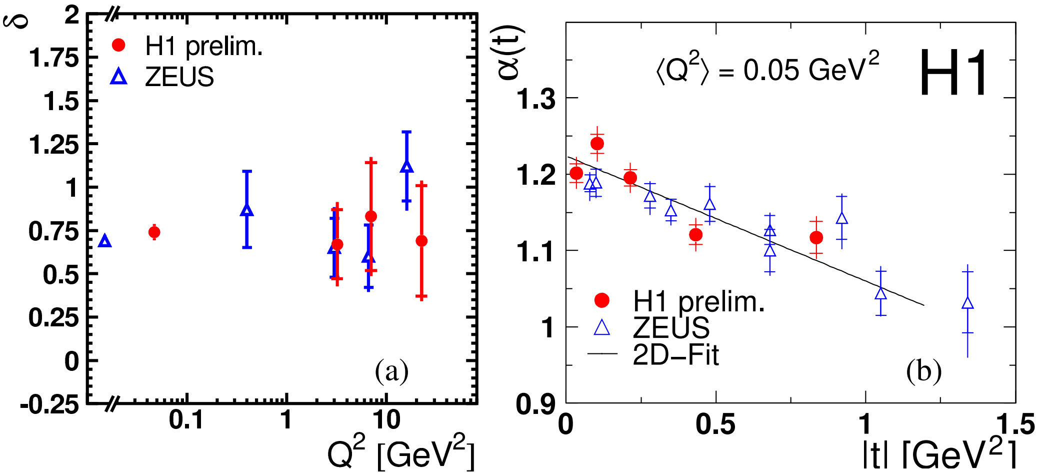

FIGURE 12. (a) The $\sigma \propto W^{\delta}$ fit parameter δ for J/ψ production as a function of Q^2. (b) The effective trajectory $\alpha_{I\!P}(t)$ as a function of t for J/ψ photoproduction.

In such a process, the hard scale provided by the mass of the involved charm quark ensures the validity of a pQCD description. This is even more so in electroproduction where Q^2 can provide a second hard scale. The Q^2 and W dependent $\gamma^* p$ cross-sections have been extracted. A steep rise with energy, $\sigma \propto W^{\delta}$, was observed with values of $\delta \simeq 0.7$ independently of Q^2 (see Fig. 12a). The effective Pomeron trajectories $\alpha_{I\!P}(t) = \alpha_{I\!P}(0) + \alpha' t$ have been extracted from the study of the doubly differential $\mathrm{d}\sigma/\mathrm{dt}$ cross-section as a function of W and t. In photoproduction (see Fig. 12b), a positive value of $\alpha' = 0.164 \pm 0.028 \pm 0.030\ \mathrm{GeV}^{-2}$ was obtained, leading to a shrinkage of the forward scattering peak, even if the effect is smaller than observed in hadron-hadron interactions. In electroproduction, within its large error, the obtained value of α' was found compatible both with the photoproduction result and zero. Finally, the helicity structure has been analyzed as a function of Q^2 and t and no evidence for a violation of SCHC has been observed. Assuming SCHC, the ratio of the longitudinal and the transverse cross sections has been extracted as a function of Q^2.

Teubner [40] has presented a model for vector meson production based on k_T factorization, which uses a parton-hadron duality ansatz to avoid the large uncertainties arising from the poorly known vector meson wave functions. The predictions obtained for J/ψ cross section as a function of W (see Fig. 13) with different sets of gluon distribution show a huge spread. This indicates a possible sensitivity to the gluon at small x and small to intermediate scales, i.e. a kinematic region where fits to the inclusive data do not constrain the gluon with high precision. Getting high precision data on vector meson production at HERA and reducing the remaining theoretical uncertainties might then allow to pin down the gluon at low x.

Kroll [41] presented a LO QCD calculation for light vector meson electroproduction taking into account the transverse momenta of the quark ant the anti-quark as well as Sudakov factors. The GPDs are modeled according to the ansatz of Radyushkin and Gaussian wavefunctions are used for the vector mesons. A fair agreement with the available data on ρ^0 and ϕ production at HERA is obtained between the predictions for

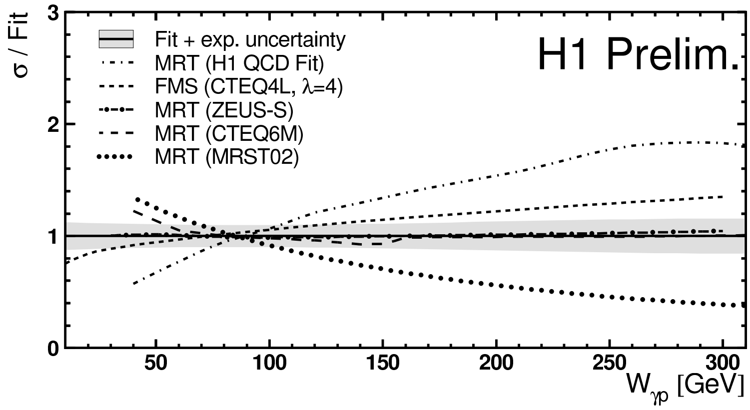

FIGURE 13. Ratio versus W of the MRT [40] theoretical predictions based on several gluon distributions to a parametrization of H1 J/ψ photoproduction preliminary data.

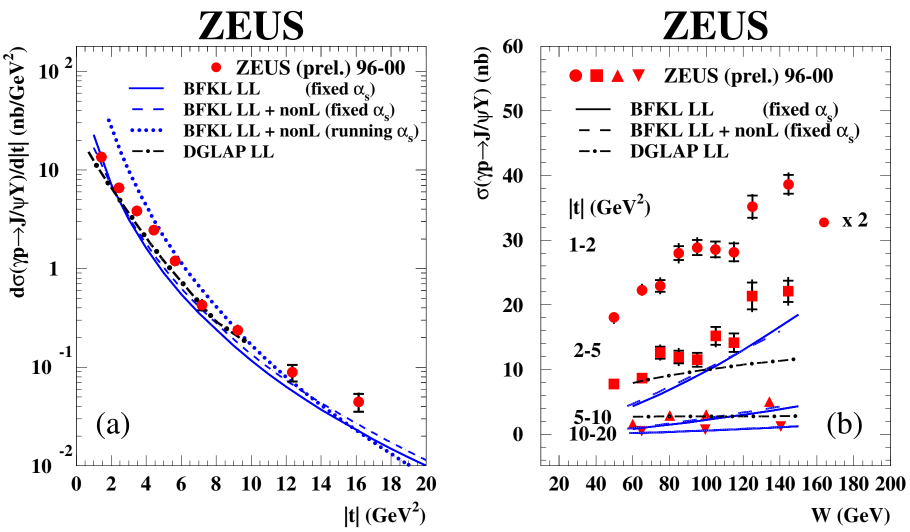

FIGURE 14. The proton-dissociative diffractive photoproduction of J/psi mesons cross sections for $|t| > 1$ GeV^2 (a) as a function of t and (b) as a function of W for four bins in t compared to predictions from based on BFKL and DGLAP.

the transverse and the longitudinal cross section as well as for the spin density matrix elements.

Photoproduction of vector mesons at large $|t|$ is largely studied since a few years as it is expected to be described by perturbative models involving the BFKL dynamics in the exchanged gluon ladder [42]. These models predict a power law behavior of the t dependence of the cross section and a rise with $|t|$ of the steepness of the W dependence.

H1 has presented [43] results on ρ^0 photoproduction in the kinematic range $75 < W < 95$ GeV and $1.5 < |t| < 10$ GeV^2 where the mass of the proton dissociative system Y is limited to $M_Y < 5$ GeV. The measured t dependence of the cross-section is well described by a power law of the form $|t|^{-n}$ with $n = 4.41 \pm 0.07^{+0.07}_{-0.10}$ and can

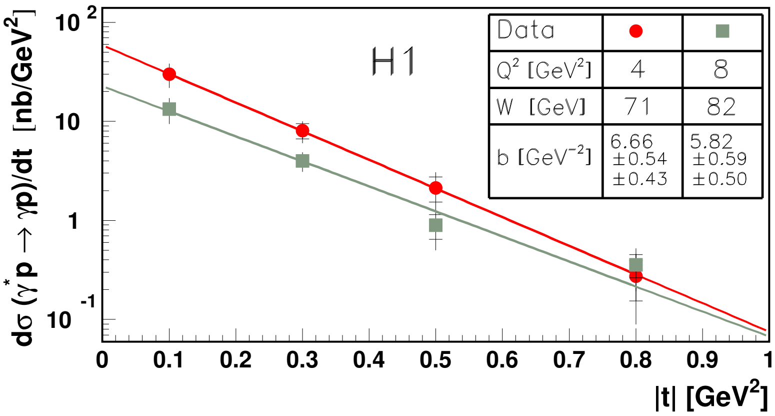

FIGURE 15. The DVCS cross section differential in t, for $Q^2 = 4$ GeV^2 at $W = 71$ GeV and for $Q^2 = 8$ GeV^2 at $W = 82$ GeV as measured by H1. The lines represent the results of fit of the form e^{-bt}.

be reproduced by BFKL model predictions. A study of the helicity structure has been performed and confirms the violation of SCHC in the case of ρ^0 photoproduction at large $|t|$ in contrast to what was observed for high $|t|$ J/ψ production [44, 45]. This is generally attributed to differences in the wave function between ρ and J/ψ.

J/ψ photoproduction at large $|t|$ has been studied by ZEUS [46] in the kinematic range $50 < W < 150$ GeV, $|t| > 1$ GeV^2 and $M_Y < 30$ GeV. Both the t dependence and the W dependence of the cross-section have been extracted, as shown on Fig. 14. Fits of the form W^δ to the W dependence of the cross section lead to values of $\delta \simeq 1$ with an indication for a rise of δ with $|t|$. The model based on BFKL has been found to describe the t dependence.

The opportunity to study Generalized Parton Distributions (GPDs) was discussed in a common session with the Spin Physics working group. Information about GPDs in lepton nucleon scattering can be provided by measurements of exclusive processes in which the nucleon remain intact. The simplest process sensitive to GPDs is Deeply Virtual Compton Scattering (DVCS), i.e. exclusive photon production off the proton $\gamma^* p \longrightarrow \gamma p$ at small $|t|$ but large Q^2, which is calculable in perturbative QCD. Such a final state also receives contributions from the purely electromagnetic Bethe-Heitler process, where the photon is radiated from the lepton. The resulting interference term in the cross section vanishes as long as one integrates over the azimuthal angle between the lepton and the hadron plane. It is then possible to extract the DVCS cross section by subtracting the Bethe-Heitler contribution, as done by H1 and ZEUS. The azimuthal asymmetries resulting from the interference are also sensitive to GPDs and are studied by HERMES, COMPASS and at JLAB. Extracting GPDs from the DVCS process would allow, through the Ji's sum rule, to determine the total angular momentum carried by the quarks which contribute to the proton spin.

A new high statistics analysis of DVCS has been performed by the H1 experiment [47] in the kinematic region $2 < Q^2 < 80$ GeV^2, $30 < W < 140$ GeV and $|t| < 1$ GeV^2. The $\gamma^* p \longrightarrow \gamma p$ cross section has been measured as a function of Q^2 and as a function of W. The W dependence can be parametrised as $\sigma \propto W^\delta$, yielding $\delta = 0.77 \pm 0.23 \pm 0.19$ at

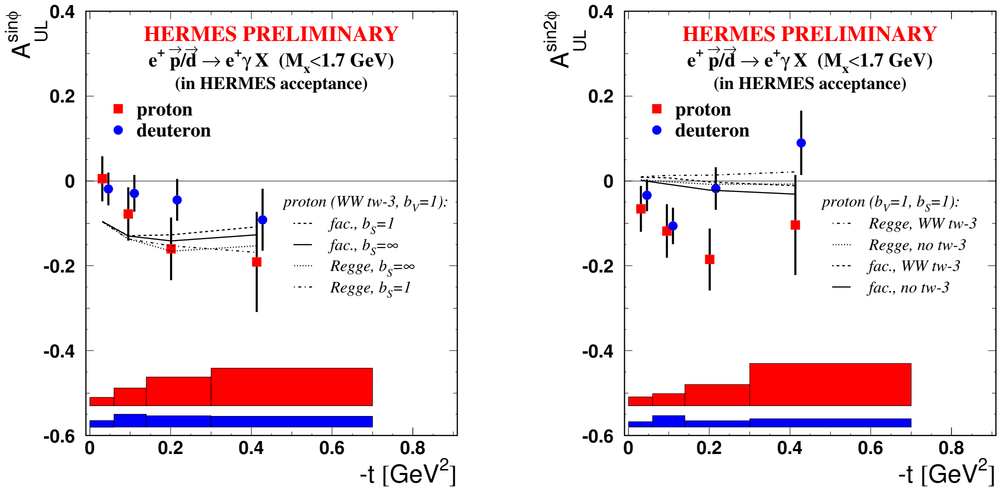

FIGURE 16. The $\sin\phi$ and $\sin 2\phi$ moments of longitudinal target-spin asymmetry on hydrogen and deuterium as function of t as measured by HERMES compared to predictions based on GPDs.

$Q^2 = 8$ GeV^2, i.e. a value similar to J/ψ production indicating the presence of a hard scattering process. For the first time, the DVCS cross section has been measured differentially in t (see Fig. 15) and the observed fast decrease with $|t|$ can be described by the form $e^{-b|t|}$ with $b = 6.02 \pm 0.35 \pm 0.39$ GeV^2 at $Q^2 = 8$ GeV^2. This measurement allows to further constrain the models, as their normalization depends directly on the t slope parameter. NLO QCD calculations using a GPD parametrization based on the ordinary parton distributions in the DGLAP region and where the skewedness is dynamically generated provide a good description of both the Q^2 and the W dependences.

A review of the HERMES results on DVCS [48] has been presented, including new data on polarized targets. On basis of unpolarized target data, one can measure the beam charge asymmetries, which are sensitive to the real part of the DVCS amplitudes, and the beam spin asymmetries, which are sensitive to the imaginary part. These are in fact mainly sensitive to the H GPD. Both asymmetries have been extracted and show the expected $\cos(\phi)$ and $\sin(\phi)$ behavior, respectively. A measurement of the t dependence of the beam charge asymmetry has been performed and comparison with models indicate the possible sensitivity of the data to constrain GPDs. Polarized target have been analyzed and the longitudinal target spin asymmetry, which is sensitive to the $\tilde{H}$ GPD, has been measured for the fist time. The resulting $\sin(\phi)$ and $\sin(2\phi)$ moments are shown as a function of t in Fig. 16, together with prediction based on GPD models. The sizeable $\sin(2\phi)$ moment might indicate a sensitivity to the twist-3 H and $\tilde{H}$ contributions. The installation of a new recoil detector will allow to tag directly the final state proton and to reduce the uncertainties due to the backgrounds arising from the missing mass techniques used up to now to guarantee exclusivity.

Gavalian [49] summarized the previous results on DVCS obtained by the CLAS experiment at JLAB, which measured in particular the beam spin asymmetry. In 2004 a dedicated DVCS experiment has been operated in Hall A and new results are expected soon. He also reviewed the status of the upgrade of the CLAS experiment which would allow to measure DVCS with the expected 12 GeV beam.

Exclusive meson production processes provide as well access to GPDs. HERMES has studied [50] exclusive π^+ production which is sensitive to the $\tilde{H}$ and the $\tilde{E}$ GPDs. The Q^2 dependent cross section has been measured and found to be in good agreement with a GPDs based model. A first measurements of the target spin asymmetry for ρ^0 production, which probes the E GPD, has been performed.

Weiss [51] reviewed the theoretical status of hard electroproduction of pions and kaons and their link to GPDs.

TOWARDS THE LHC

Diffractive physics has provided a rich source of important results from both HERA and the TEVATRON. Within the past few years there has been increasing interest to the study of diffractive processes at the LHC in connection with the proposal to add forward proton detectors to the LHC experiments. Various aspects of physics with forward proton tagging at the LHC have been under discussion in our working group.

Eggert [52] described the status of the TOTEM detector and the prospects of measurements of total and elastic pp - cross section. In particular, the total pp - cross section will be measured with the record (order 1 %) accuracy. This would allow to strongly restrict the range of existing theoretical models. Elastic cross section will be measured in the wide interval of momentum transfer $10^{-3} < -t < 8$ GeV^2.

The measurement of the elastic slope $b(t = 0)$ at the LHC is especially important, since it is expected (see for example [53, 54]) that this quantity is much more sensitive to the effects of the multi-Pomeron cuts than the total cross section.

Studies of diffractive physics at TOTEM require integration with CMS. CMS and TOTEM together will provide the largest acceptance detector ever built at a hadron collider. From the point of view of testing different regimes of the asymptotical behavior of the pp -scattering amplitude, it will be very informative to measure accurately the survival probabilities of one, two, three (maybe even four) rapidity gaps [55, 56, 57]. CMS/TOTEM physics menu will include also measurements of the centrally produced low mass systems (χ -bosons, dijets, diphotons). Special attention in his talk Eggert paid to the new ($\beta*$ =172m) optics aimed at optimization of diffractive proton detection at L= 10^{32}cm^{-2}s^{-1}.

Several speakers (Albrow, Cox, Kowalski, Piotrzkowski and Royon) discussed the unique physics potential of forward proton tagging at 420m at the LHC. The use of forward proton detectors as a means to study Standard Model (SM) and New Physics at the LHC has only been fully appreciated within the last few years, (see e.g. [57, 58] and references therein). By detecting protons that have lost less than 2 % of their longitudinal momentum, a rich QCD, electroweak, Higgs and BSM program becomes accessible, with a potential to study phenomena which are unique at the LHC, and difficult even at a future linear collider [59, 60, 61, 62, 63].

It was emphasized by Albrow, Cox and Royon [64] that the so-called central exclusive production (CEP) process might provide a particularly clean environment to search for, and identify the nature of, new particles at the LHC. There is also a potentially rich, more

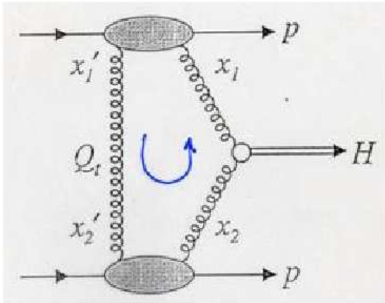

FIGURE 17. Schematic diagram for central exclusive Higgs production at the LHC, $pp \to p + H + p$.

exotic physics menu including (light) gluino and squark production, gluinonia, radions, and indeed any object which has 0^{++} or 2^{++} quantum numbers and couples strongly to gluons [57].

By central exclusive, we refer to the process $pp \to p \oplus \phi \oplus p$, where the symbol meaning has been described in the section "Diffraction at the TEVATRON". The process is attractive for two main reasons. Firstly, if the outgoing protons remain intact and scatter through small angles, then, to a very good approximation, the central system ϕ must be dominantly produced in a spin 0, CP even state, therefore allowing a clean determination of the quantum numbers of any observed resonance. Secondly, as a result of these quantum number selection rules, coupled with the (in principle) excellent mass resolution on the central system achievable if suitable proton detectors are installed, signal to background ratios greater than unity are predicted for SM Higgs production [65], and significantly larger for the lightest Higgs boson in certain regions of the MSSM parameter space [66]. Simply stated, the reason for these large signal to background ratios is that exclusive b quark production, the primary background in light Higgs searches, is heavily suppressed due to the quantum number selection rules. Another attractive feature is the ability to directly probe the CP structure of the Higgs sector by measuring azimuthal asymmetries in the tagged protons [67]. Another strategy to explore the manifestation of the explicit CP violation in the Higgs sector was recently studied by Ellis et al. [68].

The 'benchmark' CEP process for new physics searches is SM Higgs production, sketched in Fig. 17. The cross section prediction for the production of a 120 GeV Higgs at 14 TeV is 3 fb, falling to 1 fb at 200 GeV [27] [1] The simplest channel to observe the SM Higgs in the tagged proton approach from the experimental perspective is the WW decay channel [60, 69]. More challenging from a trigger perspective in the $b\bar{b}$ channel. This mode, however, becomes extremely important in the so-called 'intense coupling regime' of the MSSM, where the CEP is likely to be the discovery channel. In this case it is expected close to 10^3 exclusively produced double-tagged Higgs bosons in 30fb^{-1} of delivered luminosity. About 100 would survive the experimental cuts, with a signal-to-background ratio of order 10.

[1] for the discussion of the uncertainties in this calculation, see [66].

Furthermore, as was reported in [32, 33, 63], forward proton tagging will make possible a unique program of high-energy photon interactions physics at the LHC. For example, the two-photon production of W pairs will allow a high precision study of the quartic gauge couplings [63]. Photon interactions are enhanced in heavy ion collisions and studies of such ultra-peripheral collisions were discussed in [32, 33]. In addition, two-photon exclusive production of lepton pairs provides an excellent tool for calibrating both luminosity and the energy scale of the tagged events [63].

Finally, by tagging both outgoing protons, the LHC is effectively turned into a glue-glue collider. This will open up a rich, high rate QCD physics menu (especially in what concerns diffractive phenomena), allowing to study the skewed unintegrated gluon densities and the details of rapidity gap survival [62]. Note that the CEP provides a source of practically pure gluon jets (gluon factory [72]). This can be an ideal laboratory to study the properties of gluon jets, especially in comparison with the quark jets, and even the way to search for the glueballs.

Cox and Kowalski [60, 62] discussed the outline of the FP420 R&D project aimed at assessing whether it is possible to install forward proton detectors with appropriate acceptance at ATLAS and/or CMS, and to fully integrate such detectors within the experimental trigger frameworks [61].

REFERENCES

1. P.D.B. Collins, *An Introduction to Regge Theory and High Energy Physics,* Cambridge University Press, Cambridge, 1977.
2. ZEUS Coll., S. Chekanov et al, Eur. Phys. J C 38 (2004) 43.
3. K. Goulianos, arXiv:hep-ph/0407035.
4. K. Golec Biernat, J. Kwiecinski and A. Szczurek, Phys. Rev. D 56 (1997) 3995.
5. paper 980 submitted to ICHEP 2002; paper 981 submitted to ICHEP 2002; paper 5-090 submitted to EPS 2003.
6. DESY-05-011, to be published in Nucl. Phys. B.
7. ZEUS Coll., S. Chekanov et al, Eur. Phys. J C 25 (2002) 169.
8. paper 984 submitted to ICHEP 2002.
9. P. Laycock, these Proceedings.
10. A. Levy, these Proceedings.
11. J.C. Collins. Phys. Rev. D 557 (1998) 3051; [erratum-ibid. Phys. Rev. D 61 (2000) 019902].
12. V.N. Gribov and L.N. Lipatov., Sov. J. Nucl. Phys. 15 (1972) 438; Yu.L. Dokshitzer, Sov. Phys. JETP 46 (1977) 641; G. Altarelli and G. Parisi, Nucl. Phys. B 126 (1977) 298.
13. A. Martin, these Proceedings and references therein.
14. M. Beckingham, these Proceedings; paper 6-178 submitted to ICHEP 2004.
15. M. Mozer, these Proceedings; paper 6-177 submitted to ICHEP 2004.
16. P. Laycock, these Proceedings; paper 6-821 submitted to ICHEP 2004.
17. L. Adamczyk, these Proceedings; paper 6-0229 submitted to ICHEP 2004.
18. CDF Coll., T. Affolder et al., Phys. Rev. Lett. 84 (2000) 5043.
19. A.B. Kaidalov et al., Eur. Phys. J. C 21 (2001) 521.
20. A.B. Kaidalov et al., Phys. Lett. B 559 (2003) 235.
21. A.B. Kaidalov et al., Phys. Lett. B 567 (2003) 61.
22. M. Klasen and G. Kramer, DESY-04-011, arXiv:hep-ph/0401202; M. Klasen and G. Kramer, Eur. Phys. J. C 38 (2004) 93.
23. R. Renner, these Proceedings; paper 6-0259 submitted to ICHEP 2004.
24. ZEUS Coll., S. Chekanov et al., Eur. Phys. J. C 23 (2002) 615.
25. M. Klasen, these Proceedings; arXiv:hep-ph/0506121.
26. D. Bodeker et al., Z. Phys. C 63 (1994) 471.

27. V. A. Khoze, A. D. Martin and M. G. Ryskin, Eur. Phys. J. C 14 (2000) 525.
28. K. Goulianos, these Proceedings.
29. A.B. Kaidalov et al., arXiv:hep-ph/0409258.
30. V.A.Khoze et al., arXiv:hep-ph/0507040.
31. W. Guryn, these Proceedings.
32. S. White, these Proceedings.
33. S.Klein, these Proceedings.
34. S. Brodsky, these Proceedings.
35. E. Levin, these Proceedings.
36. J. R. Andersen, these Proceedings.
37. N. d'Hose, these Proceedings.
38. ZEUS Coll., S. Chekanov et al., Nucl. Phys. B 718 (2005) 3.
39. C. Kiesling, these Proceedings.
40. T. Teubner, these Proceedings.
41. P. Kroll, these Proceedings.
42. R. Enberg, J. R. Forshaw, L. Motyka and G. Poludniowski, JHEP 0309 (2003) 008
G. G. Poludniowski, R. Enberg, J. R. Forshaw and L. Motyka, JHEP 0312 (2003) 002 [arXiv:hep-ph/0311017].
43. C. Gwilliam, these Proceedings.
44. H1 Coll., A. Aktas et al., Phys. Lett. B 568 (2003) 205.
45. ZEUS Coll., S. Chekanov et al., Eur. Phys. J. C 26 (2003) 389.
46. D. Szuba, these Proceedings.
47. S. Glazov, these Proceedings.
H1 Coll., A. Aktas et al., arXiv:hep-ex/0505061.
48. M. Koputin, these Proceedings.
49. G. Gavalian, these Proceedings.
50. A. Vandenbroucke, these Proceedings.
51. C. Weiss, these Proceedings.
52. K. Eggert, these Proceedings.
53. V. A. Khoze, A. D. Martin and M. G. Ryskin, Nucl. Phys. B (Proc. Suppl.) 99 (2001) 213.
54. V. A. Khoze, A. D. Martin and M. G. Ryskin, Eur. Phys. J. C 18 (2000) 167.
55. K. Goulianos, Phys. Lett. B 358 (1995) 379.
56. K. Goulianos, these Proceedings.
57. V. A. Khoze, A. D. Martin and M. G. Ryskin, Eur. Phys. J. C 23 (2002) 311;
M.G. Ryskin, A. D. Martin and V.A. Khoze, arXiv:hep-ph/0506272;
58. B. Cox, arXiv:hep-ph/0409144.
59. M. Albrow, these Proceedings.
60. B. Cox, these Proceedings.
61. FP-420 :M. Albrow et al., CERN-LHCC-2005-025, LHCC-I-015.
62. H. Kowalski, these Proceedings.
63. K. Piotrzkowski, these Proceedings.
64. C. Royon, these Proceedings.
65. A. De Roeck, V. A. Khoze, A. D. Martin, R. Orava and M. G. Ryskin, Eur. Phys. J. C 25 (2002) 391.
66. A. B. Kaidalov, V. A. Khoze, A. D. Martin and M. G. Ryskin, Eur. Phys. J. C 33 (2004) 261.
67. V. A. Khoze, A. D. Martin and M. G. Ryskin, Eur. Phys. J. C 34 (2004) 327.
68. J. R. Ellis, J.S.Lee and A. Pilaftsis, Phys.Rev. **D71** (2005) 075007.
69. B. E. Cox et al., arXiv:hep-ph/0505220.
70. V. A. Khoze, A. D. Martin and M.G.Ryskin, Phys. Lett. B401 (1997) 30.
71. V. A. Khoze, A. D. Martin and M. G. Ryskin, arXiv:hep-ph/0006005, In Proc. of 8th Int. Workshop on Deep Inelastic Scattering and QCD (DIS2000), Liverpool, eds. J.Gracey and T.Greenshaw (World Scientific, 2001), p.592.
72. V. A. Khoze, A. D. Martin and M. G. Ryskin, Eur. Phys. J. C 19 (2001) 477; Erratum: ibid. C 20 (2001) 599.
73. A. B. Kaidalov, V. A. Khoze, A. D. Martin and M.G.Ryskin, Eur. Phys. J. C 31 (2003) 387.